

Infection of the Upper Respiratory Tract of Hamsters by the Bovine Parainfluenza Virus Type 3 BN-1 Strain Expressing Enhanced Green Fluorescent Protein

Takashi Ohkura, ^{a*} Moeko Minakuchi, ^a Mami Sagai, ^a Takehiro Kokuho, ^b Misako Konishi, ^c Ken-ichiro Kameyama, ^c and Kaoru Takeuchi^a

Laboratory of Environmental Microbiology, Faculty of Medicine, University of Tsukuba, ^a Biologics Production, Center for Animal Disease Control and Prevention, ^b Viral Disease and Epidemiology Research Division, ^c National Institute of Animal Health, Tsukuba, Ibaraki, Japan

*Present address: Takashi Ohkura, Department of Molecular Biosciences, Northwestern University, Evanston, Illinois, USA

Words in abstract: 147

Words in main text: 3182

Number of figures and tables: 8

Number of references: 22

Running title: PARAINFLUENZA VIRUS TROPISM IN HAMSTERS

Address correspondence to Kaoru Takeuchi, ktakeuch@md.tsukuba.ac.jp

ABSTRACT

Bovine parainfluenza virus type 3 (BPIV3) is an important pathogen associated with bovine respiratory disease complex (BRDC). We have generated a recombinant BPIV3 expressing enhanced green fluorescent protein (rBPIV3-EGFP) based on the BN-1 strain isolated in Japan. After intranasal infection of hamsters with rBPIV3-EGFP, EGFP fluorescence was detected in the upper respiratory tract including the nasal turbinates, pharynx, larynx, and trachea. In the nasal turbinates, rBPIV3-EGFP attained high titers ($> 10^6$ TCID₅₀/g of tissue) 2 to 4 days after infection. Ciliated epithelial cells in the nasal turbinates and trachea were infected with rBPIV3-EGFP. Histopathological analysis indicated that mucosal epithelial cells in bronchi were shed by 6 days after infection, leaving non-ciliated cells, which may have increased susceptibility to bacterial infection leading to the development of BRDC. These data indicate that rBPIV3-EGFP infection of hamsters is a useful small animal model for studying the development of BPIV3-associated BRDC.

INTRODUCTION

Bovine parainfluenza virus type 3 (BPIV3), a member of the genus *Respirovirus* in the family *Paramyxoviridae*, is an enveloped virus with a non-segmented negative-sense RNA genome (Karron and Collins, 2013). BPIV3 is one of the most important viruses associated with bovine respiratory disease complex (BRDC), commonly referred as “Shipping fever”, in cattle (Autio et al., 2007; Snowden et al.,

2007). The BPIV3 genome encodes six structural proteins: the nucleocapsid (N), phosphoprotein (P), matrix (M), fusion (F), hemagglutinin-neuraminidase (HN), and large (L) proteins. The P gene also encodes three accessory proteins, the C, V and D proteins. The C protein is translated from an alternative translation initiation site resulting in a different reading frame, and the V and D proteins are translated from edited mRNAs. Two envelope glycoproteins, the HN and F proteins, mediate receptor binding and membrane fusion, respectively. Therefore, the HN protein is primarily responsible for determining the tropism of BPIV3 (Karron and Collins, 2013).

The HN protein recognizes sialic acid-containing cellular glycoconjugates. Although the fine structure of sialic-acid residues that bind the HN protein of BPIV3 have not yet been reported, those that bind to the HN protein of the closely related human parainfluenza type 3 virus (HPIV3) have been reported (Amonsens et al., 2007; Fukushima et al., 2014; Suzuki et al., 2001; Zhang et al., 2005). In a cell-based assay using an *in vitro* model of human airway epithelium and neuraminidases specific for α 2-6-linked or α 2-3-/ α 2-8-linked sialic acid residues, HPIV3 was reported to utilize α 2-6-linked sialic acid residues for initiating infection (Zhang et al., 2005). On the other hand, in a non-cell-based assay using purified gangliosides, HPIV3 was reported to bind to both α 2-3- and α 2-6-linked sialic acid residues (Fukushima et al., 2014; Suzuki et al., 2001). In another non-cell-based assay using the glycan array of the Consortium for Functional Glycomics, HPIV3 was reported to bind α 2-3-linked sialic acid residues (Amonsens et al., 2007). In addition, another study reported that HPIV3 also utilized heparin sulfate moieties on the cell surface (Bose and Banerjee, 2002).

Thus, the receptor specificity of HPIV3 and BPIV3 is still controversial.

For the pathogenesis of BPIV3, only limited studies of its pathogenesis in calves have been reported (Tsai and Thomson, 1975; Van der Maaten, 1969b). This virus also infects rhesus monkeys, chimpanzees, and humans, although replication is limited and restricted to the respiratory tract in those hosts (Karron and Collins, 2013). Hamsters are often used as small models for studying BPIV3 tropism (Van der Maaten, 1969a) and for evaluating the efficacy of recombinant BPIV3 vaccines (Haller et al., 2000; Schmidt et al., 2001). BPIV3 replicates in the respiratory tracts, but the systemic infection and the exact cell tropism of BPIV3 in hamsters have not yet been reported.

EGFP-expressing reporter viruses have been successfully used to study the cell tropism and pathogenesis of paramyxoviruses with high sensitivity (de Swart et al., 2007; Takeuchi et al., 2012; von Messling et al., 2004). In our study, we examined the tropism and pathogenesis of BPIV3 in hamsters using the enhanced green fluorescent protein (EGFP)-expressing BPIV3 (rBPIV3-EGFP). We found that rBPIV3-EGFP efficiently replicated in the nasal turbinates, pharynx, larynx, and trachea of hamsters. Ciliated epithelial cells in the nasal turbinates and trachea were infected. In addition, rBPIV3-EGFP caused mucosal epithelial cell shedding in the bronchi. These data are important for understanding the pathogenesis of BPIV3 and BPIV3-associated BRDC.

RESULTS

Construction of the full-length BPIV3 cDNA and rescue of rBPIV3 and rBPIV3-EGFP.

An infectious full-length antigenomic cDNA of BPIV3-BN-1 strain was constructed by RT-PCR amplification of genomic RNA to produce three DNA segments, which were assembled in sequential cloning step, resulting in the p(+)BPIV3 (Fig. 1). As a genetic marker, an *NheI* restriction enzyme site in the HN gene was introduced in place of a *StuI* site. Recombinant BPIV3 (rBPIV3) was recovered from the p(+)BPIV3 (Fig. 1). To confirm that recovered virus was rBPIV3, PCR fragments of the HN gene of rBPIV3 and BPIV3 were analyzed for the presence of the *NheI* restriction enzyme site (Fig. 2). The 1020 bp PCR fragments derived from rBPIV3 was cleaved with *NheI* but not with *StuI*. In contrast, the PCR fragment derived from BPIV3 was cleaved with *StuI* but not with *NheI* as expected. Identification of *NheI* site demonstrated that recovered rBPIV3 was indeed derived from plasmid DNA containing the full-length rBPIV3 genome by reverse genetics.

To make recombinant BPIV3 expressing the EGFP, we introduced the EGFP gene between the N and P genes of the p(+)BPIV3, resulting in the p(+)BPIV3-EGFP. Then, infectious virus (rBPIV3-EGFP) was recovered from the p(+)BPIV3-EGFP. Repeated attempts to recover recombinant virus having the EGFP gene between the leader sequence and the N gene were not successful (data not shown).

In vitro characterization of rBPIV3 and rBPIV3-EGFP.

First, we compared the growth of BPIV3, rBPIV3 and rBPIV3-EGFP in MDBK cells (Fig. 3A). All virus strains showed similar replication kinetics and attained peak titers of 10^{10} 50% tissue culture infective dose (TCID₅₀)/ml, suggesting that rBPIV3

retained the phenotype of BPIV3 and that the EGFP gene had no obvious detrimental effect on the growth of rBPIV3-EGFP. rBPIV3-EGFP replicated and expressed EGFP in several other cell lines including CV-1, Vero, HeLa, HEp-2 and 293 cells, but did not induce syncytium formation (Fig. 3B).

Macroscopic detection of EGFP fluorescence in organs and tissues.

To examine the systemic infection of BPIV3 in hamsters, we infected hamsters with rBPIV3-EGFP. Hamsters were infected intranasally with 1×10^6 TCID₅₀ of rBPIV3-EGFP in a 100 μ l volume. No clinical signs were observed during the course of the experiment. Upon necropsy at 2 days post-infection, EGFP fluorescence was detected in the nasal turbinates and weakly in the trachea of all hamsters. On day 4, strong EGFP fluorescence was detected in the entire region of the nasal turbinates, pharynx, larynx, and trachea of all hamsters (Fig. 4). There was no expression in other tissues and organs. EGFP-expressing cells were restricted in the lumen of the trachea (Fig. 4). Unexpectedly, EGFP fluorescence was not detected in any sections of the lungs of all hamsters. By day 6, the intensity of the EGFP fluorescence had rapidly weakened in those tissues and was no longer detectable by day 8.

Growth of rBPIV3-EGFP in nasal turbinates and trachea of hamsters.

We then examined the growth of rBPIV3-EGFP in the nasal turbinates and trachea of infected hamsters. In the nasal turbinates, rBPIV3-EGFP attained very high titers ($> 10^6$ TCID₅₀/g of tissue) on days 2 and 4 post-infection (Table 1). A gradual reduction

by 1 log₁₀ was detected by day 6, and titers rapidly dropped by 3 log₁₀ by day 8 (Table 1). In the trachea, rBPIV3-EGFP attained high titers (10^{4.5} TCID₅₀/g of tissue) by day 2 and increased to very high titers (10^{5.7} TCID₅₀/g of tissue) by day 4. Titers then decreased by 2 log₁₀ by day 6 and were further reduced by 1 log₁₀ by day 8, indicating that the infection was rapidly cleared within a few days.

We could not detect efficient virus growth in the lung (Table 1), although previous reports indicated efficient virus growth in both the nasal turbinates and lungs (Haller et al., 2000; Schmidt et al., 2001). To examine whether the EGFP gene introduced in rBPIV3-EGFP attenuated virus growth in lungs, we infected hamsters with recombinant virus without the EGFP (rBPIV3). Again, rBPIV3 replicated efficiently in both the nasal turbinates (10^{6.2} TCID₅₀/g of tissue) and trachea (10^{5.0} TCID₅₀/g of tissue) but less efficiently in the lungs (10^{3.7} TCID₅₀/g of tissue) (Table 2), suggesting that the EGFP gene did not attenuate virus growth in the lungs of hamsters.

To examine whether lower numbers of virus can establish infection in hamsters, we infected hamsters with lower doses (10⁵ or 10⁴ TCID₅₀ of virus per animal) of rBPIV3-EGFP. When hamsters were infected with 10⁵ or 10⁴ TCID₅₀ of rBPIV3-EGFP, 10^{6.1} or 10^{5.5} TCID₅₀/g of tissue of virus were recovered from the trachea of hamsters, respectively (Table 2), indicating that lower doses of virus could still establish the infection in hamsters.

Ciliated epithelial cells were preferentially infected with rBPIV3-EGFP.

To identify the infected cells in the nasal turbinates and tracheas, we observed frozen

section of these tissues under a fluorescent microscope. Ciliated cells stained with cilia-specific antibody (β -tubulin IV) were found to be exclusively infected by rBPIV3-EGFP in both the nasal turbinates and trachea (Fig. 5A and B). Infection did not spread to underlying basal cells and did not induce syncytium formation between infected and uninfected cells.

Mucosal epithelial cell shedding and lymphocytic infiltration.

To examine the pathogenesis of BPIV3 in hamsters, we performed a histopathological analysis of fixed specimens of the nasal turbinates, trachea, and bronchi. On day 6, sloughed ciliated epithelial cells, cell debris, and red blood cells were observed in the lumen of the bronchi (Fig. 6). Diffuse expansions of the alveolar interstitia due to mononuclear cell infiltrates were also observed on day 6, but not observed in on days 2 or 4. Mucosal epithelial cells shed by day 6 post-infection left non-ciliated cells in the lumen of bronchi (Fig. 6).

DISCUSSION AND CONCLUSIONS

In this study, we have analyzed the *in vivo* tropism of BPIV3 in hamsters using EGFP-expressing recombinant BPIV3 based on the BN-1 strain. Previous studies indicated that BPIV3 replicates in the respiratory tracts of hamsters (Haller et al., 2000; Schmidt et al., 2001; Van der Maaten, 1969a), but the systemic infection and the exact cell tropism of BPIV3 were not examined. We observed EGFP expression in the entire region of the nasal turbinates, pharynx, larynx, and trachea (Fig. 3). In particular, we

detected high titers of virus ($> 10^6$ TCID₅₀/g of tissues) on days 2 and 4 post-infection in the nasal turbinates (Table 1). These titers were equivalent or 10 times higher than those reported previously (Haller et al., 2000; Schmidt et al., 2001). Interestingly, rBPIV3-EGFP did not grow efficiently in the lungs of hamsters. BPIV3 strains derived from the Kansas/15626/84 strain have been reported to replicate to similar levels in the nasal turbinates and the lungs of hamsters (Haller et al., 2000; Schmidt et al., 2001), while upper respiratory tract-specific growth of BPIV3 in hamster has been reported for the SF-4 strain (Van der Maaten, 1969a). Therefore, it is likely that the differences in virus growth in the lungs in our study and in previous studies (Haller et al., 2000; Schmidt et al., 2001) may be attributed to the strains used, although our data do not exclude the possibility that the EGFP gene introduced in rBPIV3-EGFP may have some detrimental effect on virus growth in the lungs. There are 1184 nucleotide (312 amino acid) differences between the BN-1 and Kansas/15626/84 strains, including a 24-nucleotide insertion in the non-coding region in the F gene of the BN-1 strain (Ohkura et al., 2013). These nucleotide and/or amino acid differences may affect the growth of the BPIV3 in the lungs of hamsters. For virus isolation from the lungs, we routinely used small pieces of the exterior regions of the lobes, which were far from bronchi. We speculated that sloughed ciliated epithelial cells in the bronchi (Fig. 6) were not included in our specimens from the lungs.

We observed that luminal ciliated epithelial cells in the nasal turbinates and trachea were infected with rBPIV3-EGFP (Fig. 4). This observation is consistent with a previous report in which HPIV3 specifically replicated in ciliated cells of *in vitro*

reconstituted human airway epithelium (Zhang et al., 2005). Cell-cell fusion between infected cells and infection of basal cells were not observed in the trachea of hamsters (Fig. 4) as previously described (Zhang et al., 2005). We also observed a massive shedding of the ciliated cell layer in the bronchi (Fig. 6). Shedding of infected ciliated cells have been reported in the *in vitro* model of human epithelium infected with HPIV3 (Zhang et al., 2005). Mucosal epithelial cell shedding in the trachea was also reported in BPIV3-infected albino guinea pig (Shi et al., 2014). Thus, if the mucosal epithelial cell shedding also occurs in the trachea or bronchi of BPIV3-infected cattle, it would increase their susceptibility to secondary bacterial infections including *Mannheimia haemolytica* or *Pasteurella multocida*, leading to BRDC (Ackermann et al., 2000, Griffin et al., 2010).

The F protein of BPIV3 BN-1 strain has the preferred furin motif (Arg-X-Arg/Lys-Arg) at the F₁ and F₂ cleavage site, and accordingly, rBPIV3-EGFP does not require trypsin for replication in cell culture (Fig. 3). However, EGFP expression in tissues and organs other than the respiratory tracts was not observed in hamsters. It is likely that host immunity may restrict BPIV3 replication within the respiratory tract (Karron and Collins, 2013).

In summary, we investigated the systemic infection and the exact cell tropism of BPIV3 in hamsters using EGFP-expressing BPIV3. Our results reveal how infection with BPIV3 spreads within the respiratory tract of living animals after intranasal inoculation. This model is useful for studying the pathogenicity of BPIV3 and BPIV3-associated BRDC. Further studies involving infection of calves, the natural

host, with rBPIV3-EGFP will be needed to confirm the results obtained in this study.

MATERIALS AND METHODS

Cells and viruses.

Madin-Darby bovine kidney (MDBK), Vero, 293, and HeLa monolayer cell cultures were maintained in Dulbecco's modified essential medium (DMEM) supplemented with 10% fetal bovine serum (FBS) and antibiotics. HEp-2 and CV-1 monolayer cell cultures were maintained in minimal essential medium (MEM) supplemented with 10% FBS and antibiotics. The BPIV3 BN-1 strain was isolated at the National Institute of Animal Health, Japan (Inaba et al., 1963; Ohkura et al., 2013). The modified vaccinia virus Ankara (MVA-T7), which expresses the phage T7 RNA polymerase (Wyatt et al., 1995), was grown in chicken embryonic fibroblasts.

Cloning of the N, P and L genes of BPIV3 into a pGEM-3 plasmid vector.

To construct the N-expressing plasmid, the open reading frame of the N gene was synthesized from viral RNA by RT-PCR using the primers 5'-GCGAATTCATGCTGAGTCTATTTGACAC-3' and 5'-GCGAATCCTTAGTTGTTTCCAAATGCAC-3' and ligated between *EcoRI* and *BamHI* sites of the pGEM-3 plasmid, resulting in pGEM-N. To construct the P-expressing plasmid, the open reading frame of the P gene was synthesized from viral RNA by RT-PCR using the primers 5'-GCTCTAGAATGGAAAACAATGCTAAAGA-3' and

5'-GCAAGCTTTTACTGAGAGCTGACATCCT-3' and ligated between *Xba*I and *Hind*III sites of the pGEM-3 plasmid, resulting in pGEM-P. To construct the L-expressing plasmid, the open reading frame of the L gene was synthesized from viral RNA by RT-PCR using the primers 5'-GCGGTACCATGGACACCGAATCCCACAG-3' and 5'-GCGCATGCTTAATCAATATCAAATTCGT-3' and ligated between *Kpn*I and *Sph*I of the pGEM-3 plasmid, resulting in pGEM-L.

Construction of the full-length BPIV3 cDNA expressing EGFP.

To construct the full-length BPIV3 cDNA, three fragments were amplified from viral RNA by RT-PCR and assembled stepwise (Fig. 1). First, the fragment covering the BPIV3 leader sequence to the *Xho*I site at nucleotide position 2154 was amplified by RT-PCR. Then a *Bss*HIII site and the T7 promoter sequence were added by PCR using synthetic primers, resulting in the frg(*Bss*HIII-T7-*Xho*I). Second, the fragment covering from the *Nhe*I (the *Stu*I site at nucleotide position 7917 was changed to a *Nhe*I site) to the BPIV3 trailer sequence was amplified, and the genomic hepatitis delta virus ribozyme sequence and a *Not*I site were added by PCR using synthetic primers. A *Xho*I site was added just before the *Nhe*I site to join to the frg(*Bss*HIII-T7-*Xho*I), resulting in the frg(*Xho*I-Ribozyme-*Not*I). Third, the fragment covering from the *Xho*I site at nucleotide position 2154 to the *Nhe*I was amplified by RT-PCR, resulting in the frg(*Xho*I-*Nhe*I). All fragments were cloned into the pBluescriptII KS(+), whose multiple cloning site was replaced with a fragment containing *Bss*HIII and *Not*I sites,

resulting in the p(+)BPIV3. To introduce the EGFP gene between the N and P genes of the p(+)BPIV3, an extra gene unit containing a gene-start signal, a gene-end signal, an intergenic region, and *SalI/MluI* sites was inserted between the N and P gene of the p(+)BPIV3, resulting in the p(+)BPIV3-S/M. The open reading frame for the EGFP gene was amplified from the pEGFP-N1 (Clontech, Mountain View, CA) using the primers 5'-TCCTAAGATTGTCGACATGGTGAGCAAGGGCGAG-3' and 5'-GATCATCTCTACGCGTCTTACTTGTACAGCTCGTC-3' (the restriction sites are underlined) and introduced between the *SalI* and *MluI* sites of the p(+)BPIV3-S/M, resulting in the p(+)BPIV3-EGFP. All plasmids containing the full-length BPIV3 cDNA were prepared in Stbl2 cells (Life technologies, Grand Island, NY) at 30°C.

Rescue of infectious virus from p(+)BPIV3-EGFP plasmid.

HeLa cells in a 6-well plate (80% confluent) were infected with vaccinia virus MVA-T7 at a multiplicity of infection (MOI) of 1. One hour postinfection, the p(+)BPIV3 or p(+)BPIV3-EGFP plasmids (4 µg) was transfected into the MVA-T7-infected HeLa cells together with the pGEM-N, pGEM-P and pGEM-L in the presence of 10 µl of lipofectamine 2000 (Life technologies) in 250 µl of Opti-MEM (Life technologies). After a 6-hour incubation, media were replaced with DMEM supplemented with 10% FBS and antibiotics. Three days post-transfection, the supernatants were harvested and transferred onto new MDBK cell monolayers. After incubation for 3 days in the presence of 4 µg of 1-β-D-arabinofuranosylcytosine/ml, rBPIV3 and rBPIV3-EGFP were recovered from the p(+)BPIV3 and p(+)BPIV3-EGFP,

respectively.

Growth curves.

Monolayer cultures of MDBK cells in 24-well cluster plates were infected with rBPIV3 or rBPIV3-EGFP at an MOI of 0.01 and incubated at 37°C. At various times, media were harvested and the infectious titer was determined by the TCID₅₀ in MDBK cells.

Infection of hamsters with BPIV3-EGFP.

Five-week-old Syrian golden hamsters (four animals per group) were anesthetized with isoflurane and infected intranasally with 1×10^6 TCID₅₀ of rBPIV3-EGFP in a 100 µl volume. Animals were maintained separately in isolator cages. From 2 up to 8 days post-infection, animals were euthanized and the nasal turbinates, trachea and lungs (approximately 50 mg) were harvested, homogenized, and stored at -80°C. The viral titers in the tissues were determined by TCID₅₀ assay in MDBK cells. All animal experiments were performed in compliance with the guidelines of University of Tsukuba.

Macroscopic detection of EGFP fluorescence.

EGFP fluorescence in the tissues and organs of hamsters was observed using a VB-G25 fluorescence microscope equipped with a VB-7000/7010 charge-coupled device (CCD) detection system (Keyence, Osaka, Japan) or a BZ-X700 fluorescence

microscope (Keyence) equipped with a cooled CCD digital camera. Composite images with a large depth-of-field were created by extracting the pixel information from multiple Z-stack images.

Histopathological and immunohistochemical analyses.

Tissues from the nasal turbinates and trachea to bronchi were fixed in 10% phosphate-buffered formalin. Fixed tissues were embedded in paraffin, sectioned, and stained with hematoxylin and eosin. A portion of the nasal turbinates and trachea were also snap-frozen in Tissue-Tek OCT compound (Sakura Finetek, Tokyo, Japan) and incubated with a monoclonal antibody against β -tubulin IV (SIGMA, St. Louis, MO). Alexa Fluor 568-conjugated donkey anti-mouse IgG (Life technologies) was used as the secondary antibody. After a final wash, cells were mounted with Vectashield mounting medium (Vector Laboratories, Burlingame, CA), and images were acquired using a Keyence BZ-X700 fluorescence microscope equipped with a cooled CCD digital camera.

ACKNOWLEDGEMENTS

We thank B. Moss for providing the vaccinia virus MVA-T7, K. Nagata, Y. Ishii, M. Takada and R. Matsuura, H. Hikono and T. Tsuboi for their continuous support. We also thank B. He (University of Georgia) for critical reading.

This work was supported by a Grant-in-Aid (No. AGD26073) from the Ministry of Agriculture, Forestry and Fisheries of Japan.

REFERENCES

Ackermann MR, Brogden KA. 2000. Response of the ruminant respiratory tract to *Mannheimia (Pasteurella) haemolytica*. *Microbes Infect.* 2000 2:1079-88.

Amonsén M, Smith DF, Cummings RD, Air GM. 2007. Human parainfluenza viruses hPIV1 and hPIV3 bind oligosaccharides with alpha2-3-linked sialic acids that are distinct from those bound by H5 avian influenza virus hemagglutinin. *J Virol.* 81:8341-8345.

Autio T, Pohjanvirta T, Holopainen R, Rikula U, Pentikäinen J, Huovilainen A, Rusanen H, Soveri T, Sihvonen L, Pelkonen S. 2007. Etiology of respiratory disease in non-vaccinated, non-medicated calves in rearing herds. *Vet Microbiol.* 119:256-65.

Bose S, Banerjee AK. 2002. Role of heparan sulfate in human parainfluenza virus type 3 infection. *Virology.* 298:73-83.

de Swart RL, Ludlow M, de Witte L, Yanagi Y, van Amerongen G, McQuaid S, Yüksel S, Geijtenbeek TB, Duprex WP, Osterhaus AD. 2007. Predominant infection of CD150+ lymphocytes and dendritic cells during measles virus infection of macaques. *PLoS Pathog.* 3:e178. 10.1371/journal.ppat.0030178

Fukushima K, Takahashi T, Ito S, Takaguchi M, Takano M, Kurebayashi Y, Oishi K, Minami A, Kato T, Park EY, Nishimura H, Takimoto T, Suzuki T. 2014. Terminal sialic acid linkages determine different cell infectivities of human parainfluenza virus type 1 and type 3. *Virology*. 464-465:424-31. doi: 10.1016/j.virol.2014.07.033.

Griffin D, Chengappa MM, Kuszak J, McVey DS. 2010. Bacterial pathogens of the bovine respiratory disease complex. *Vet Clin North Am Food Anim Pract*. 26:381-94. doi: 10.1016/j.cvfa.2010.04.004.

Haller AA, Miller T, Mitiku M, Coelingh K. 2000. Expression of the surface glycoproteins of human parainfluenza virus type 3 by bovine parainfluenza virus type 3, a novel attenuated virus vaccine vector. *J Virol*. 74:11626-11635.

Inaba Y, Omori T, Kono M, Matsumoto M. 1963. Parainfluenza 3 virus isolated from Japanese cattle, Japan. *J. Exp. Med.* 33, 313-329

Karron RA, Collins PL, 2013. Parainfluenza viruses, p 996-1023. *In* Knipe DM, Howley PM (ed), *Fields virology*, 6th ed. Lippincott/The Williams & Wilkins Co, Philadelphia, PA.

Ohkura T, Kokuho T, Konishi M, Kameyama K, Takeuchi K. 2013. Complete Genome Sequences of Bovine Parainfluenza Virus Type 3 Strain BN-1 and Vaccine Strain BN-CE. *Genome Announc.* 1:e00247-12. doi: 10.1128/genomeA.00247-12.

Schmidt AC, McAuliffe JM, Murphy BR, Collins PL. 2001. Recombinant bovine/human parainfluenza virus type 3 (B/HPIV3) expressing the respiratory syncytial virus (RSV) G and F proteins can be used to achieve simultaneous mucosal immunization against RSV and HPIV3. *J Virol.* 75: 4594-603.

Shi HF, Zhu YM, Dong XM, Cai H, Ma L, Wang S, Yan H, Wang XZ, Xue F. 2014. Pathogenesis of a genotype C strain of bovine parainfluenza virus type 3 infection in albino guinea pigs. *Virus Res.* 188:1-7. doi: 10.1016/j.virusres.2014.03.017.

Snowder GD, Van Vleck LD, Cundiff LV, Bennett GL, Koohmaraie M, Dikeman ME. 2007. Bovine respiratory disease in feedlot cattle: phenotypic, environmental, and genetic correlations with growth, carcass, and longissimus muscle palatability traits. *J Anim Sci.* 85:1885-92.

Suzuki T, Portner A, Scroggs RA, Uchikawa M, Koyama N, Matsuo K, Suzuki Y, Takimoto T. 2001. Receptor specificities of human respiroviruses. *J Virol.* 75:4604-13.

Takeuchi K, Nagata N, Kato SI, Ami Y, Suzaki Y, Suzuki T, Sato Y, Tsunetsugu-Yokota Y, Mori K, Van Nguyen N, Kimura H, Nagata K. 2012. Wild-type measles virus with the hemagglutinin protein of the Edmonston vaccine strain retains wild-type tropism in macaques. *J Virol.* 86:3027-37. doi: 10.1128/JVI.06517-11.

Tsai KS, Thomson RG. 1975. Bovine parainfluenza type 3 virus infection: ultrastructural aspects of viral pathogenesis in the bovine respiratory tract. *Infect Immun.* 11:783-803.

Van der Maaten MJ. 1969a. Immunofluorescent studies of bovine para-influenza 3 virus. I. Cell cultures and experimentally infected hamsters. *Can J Comp Med.* 33:134-140.

Van der Maaten MJ. 1969b. Immunofluorescent studies of bovine para-influenza 3 virus. II. Experimentally infected calves. *Can J Comp Med.* 33:141-147.

von Messling V, Milosevic D, Cattaneo R. 2004. Tropism illuminated: lymphocyte-based pathways blazed by lethal morbillivirus through the host immune system. *Proc Natl Acad Sci U S A.* 101:14216-14221.

Wyatt LS, Moss B, Rozenblatt S. 1995. Replication-deficient vaccinia virus encoding bacteriophage T7 RNA polymerase for transient gene expression in mammalian cells. *Virology.* 210:202-205.

Zhang L, Bukreyev A, Thompson CI, Watson B, Peeples ME, Collins PL, Pickles RJ. 2005. Infection of ciliated cells by human parainfluenza virus type 3 in an *in vitro* model of human airway epithelium. *J Virol.* 79: 1113-1124.

FIGURE LEGENDS

Fig. 1. Construction of antigenomic cDNA of BPIV3 and BPIV3 containing the EGFP gene. The BPIV3 genome is flanked by untranslated leader (le) and trailer (tr) regions. The boxes between genes indicated the conserved gene-end sequences, intergenic sequences (IGS), and gene-start sequences. T7 promoter and Ribozyme are located upstream of the leader region (le) and downstream of the trailer region (tr), respectively. To construct the full-length BPIV3 cDNA, three fragments, frg(*Bss*HII-T7-*Xho*I), frg(*Xho*I-Ribozyme-*Not*I) and frg(*Xho*I-*Nhe*I), were amplified from viral RNA by RT-PCR and assembled stepwise, resulting in p(+)*BPIV3*. An *Nhe*I restriction enzyme site in the HN gene of p(+)*BPIV3* was used as a genetic marker and is indicated. The EGFP gene (hatched box) was inserted between the N and P genes. The nucleotide sequence between the N and P genes of the p(+)*BPIV3* and the nucleotide sequences between the N and EGFP and between the EGFP and P genes of the p(+)*BPIV3*-EGFP are indicated.

Fig. 2. Identification of the genetic marker in the recovered r*BPIV3* genome. PCR fragments, 1020 bp in length, were amplified by RT-PCR from cells infected with r*BPIV3* or *BPIV3*. The amplified region contained viral sequences from nt 7680 to 8700 in the HN gene were digested with *Nhe*I or *Stu*I. The digested and undigested PCR fragments were analyzed on a 1% agarose gel.

Fig. 3. Growth of BPIV3, rBPIV3 and rBPIV3-EGFP in MDBK cells and dissemination of rBPIV3-EGFP in cultured cell lines. (A) Replication kinetics of BPIV3, rBPIV3 and rBPIV3-EGFP. MDBK cells were infected with BPIV3 (open circles), rBPIV3 (filled circles) or rBPIV3-EGFP (triangles) at an MOI of 0.01. Media were harvested at days 0, 1, 2, 3, 4, and 5, and infectious titers were assessed as TCID₅₀ using MDBK cells. The data presented the mean ± the standard deviations of triplicate samples. (B) MDBK, CV-1, Vero, HeLa, HEp-2 and 293 cells were infected with rBPIV3-EGFP. The rBPIV3-EGFP-infected cells were visualized with EGFP autofluorescence at day 2 post-infection. Photomicrographs of EGFP fluorescence and phase contrast are shown.

Fig. 4. EGFP fluorescence in the upper respiratory tracts of hamsters after experimental infection with rBPIV3-EGFP. At day 4 post-infection, rBPIV3-EGFP infection in hamsters was detected using a Keyence VB-25 fluorescence microscope. The skull of the hamster was cut in sagittal plane (a, b, and c). Photographs were taken under daylight (a), ultraviolet light (b and d), or both (c). NT, nasal turbinates; PH, pharynx; LA, larynx; TR, trachea. Infection with rBPIV3-EGFP in the trachea was detected using a Keyence BZ-X700 fluorescence microscope (e and f). The luminal surface of trachea was infected with rBPIV3-EGFP.

Fig. 5. Infection of ciliated cells in the nasal turbinate and trachea by rBPIV3-EGFP. The nasal turbinate and trachea obtained from a hamster infected with

rBPIV3-EGFP at day 4 post-infection were investigated by immunofluorescence staining. Frozen sections of the nasal turbinate (A) and trachea (B) were observed by phase contrast and EGFP expression or stained with antibody against β -tubulin IV. DAPI was used to identify nuclei. No cell-to-cell fusion was observed between rBPIV3-EGFP-infected cells.

Fig. 6. Bronchi sections from infected hamsters after hematoxylin and eosin (H&E) staining. (A) Mucosal ciliated epithelial cell shedding (arrows) and lymphocytic infiltration (arrowheads) in the bronchi section of one hamster at day 6 post-infection. (B) Blood cells and amorphous debris in the bronchial lumen. (C) High-magnification image of the boxed area (c) in (A). (D) High-magnification image of the boxed area (d) in (B). (E) High-magnification image of the boxed area (e) in (A). (F) High-magnification image of another bronchi section of infected hamster. Non-ciliated cells (asterisk) induced by mucosal ciliated cell shedding. Bar = 100 μ m.

Table 1

Replication of rBPIV3-GFP in the upper and lower respiratory tracts of hamsters

Days post infection	Mean virus titer \pm SE log ₁₀ TCID ₅₀ /g of tissue)		
	Nasal turbinates	Trachea	Lungs
2	6.8 \pm 0.2	4.5 \pm 0.2	ND
4	6.7 \pm 0.8	5.7 \pm 0.5	<3.1
6	5.7 \pm 0.7	3.4 \pm 0.8	ND
8	<3.1	<3.1	ND

ND, not determined.

Table 2

Replication of rBPIV3 and rBPIV3-EGFP in the upper and lower respiratory tracts of hamsters on day 4 post-infection

Virus	Mean virus titer \pm SE log ₁₀ TCID ₅₀ /g of tissue)		
	Nasal turbinates	Trachea	Lungs
rBPIV3	6.2 \pm 0.2	5.0 \pm 1.0	3.7 \pm 1.4
rBPIV3-EGFP (1 \times 10 ⁵)	ND	6.1 \pm 0.4	ND
rBPIV3-EGFP (1 \times 10 ⁴)	ND	5.5 \pm 0.2	ND

ND, not determined.

FIG. 1

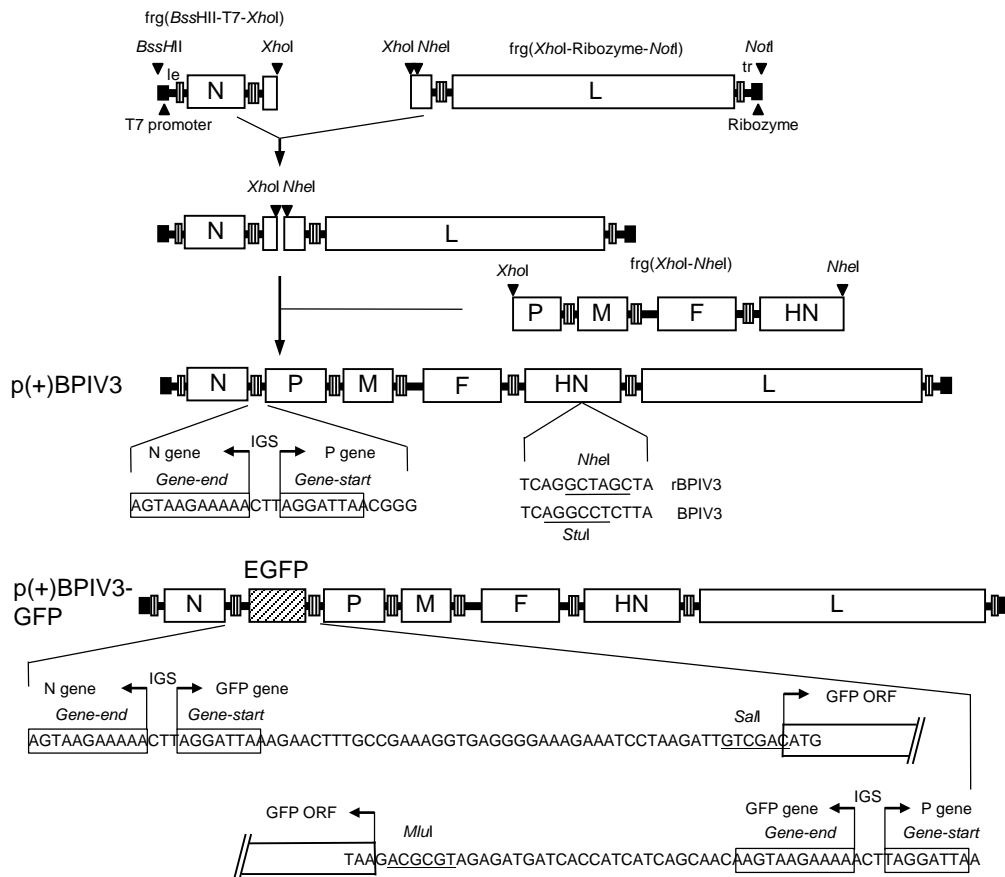


FIG.2

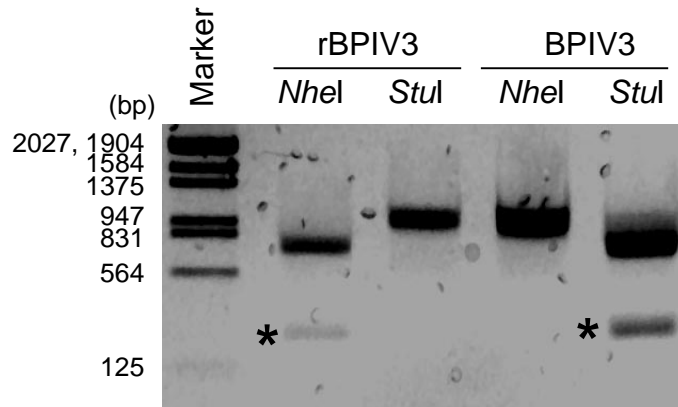
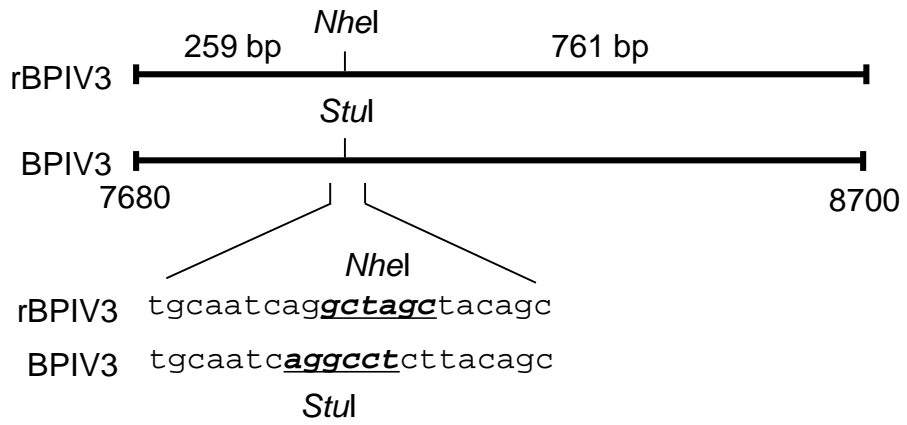
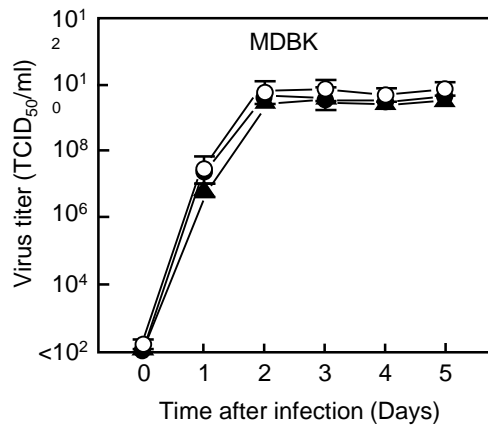


FIG.3

A



B

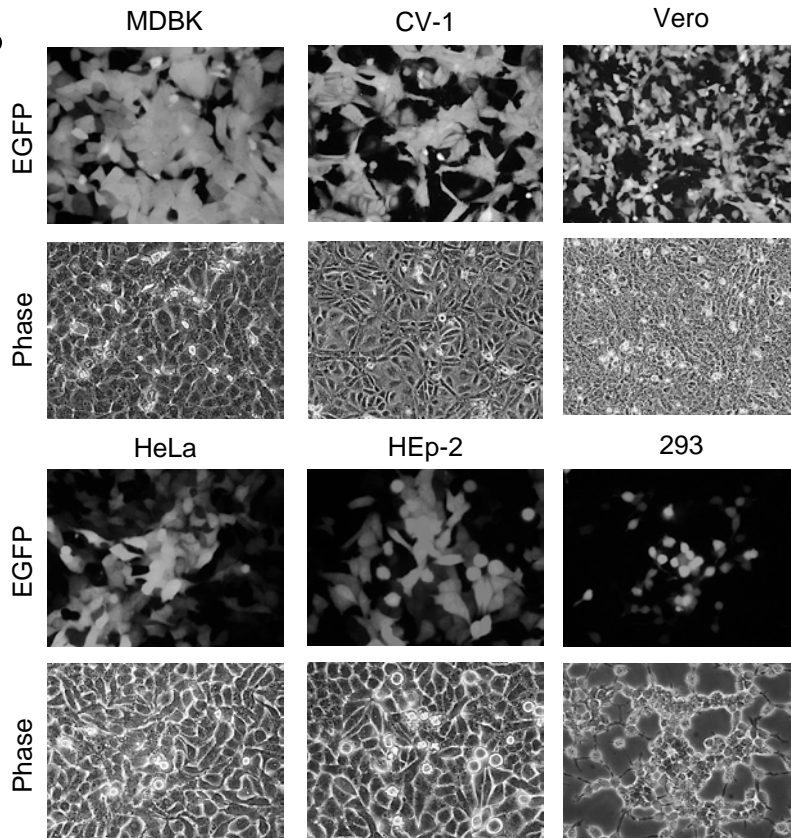
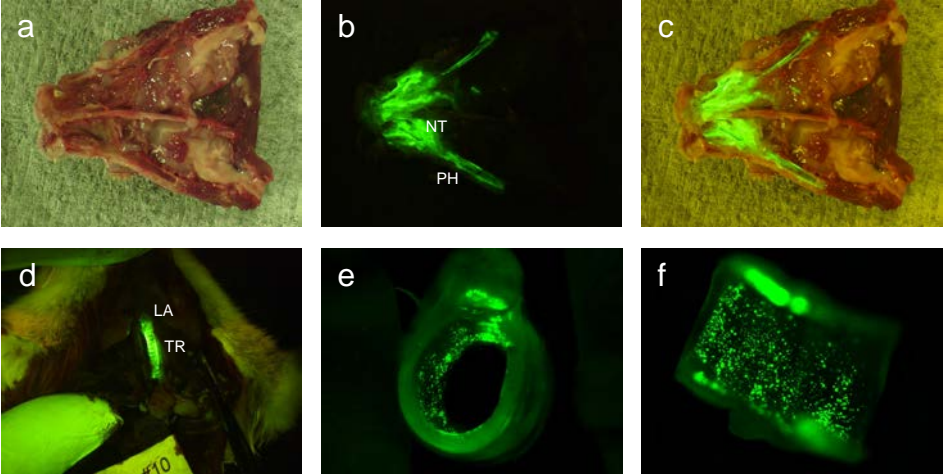


FIG.4



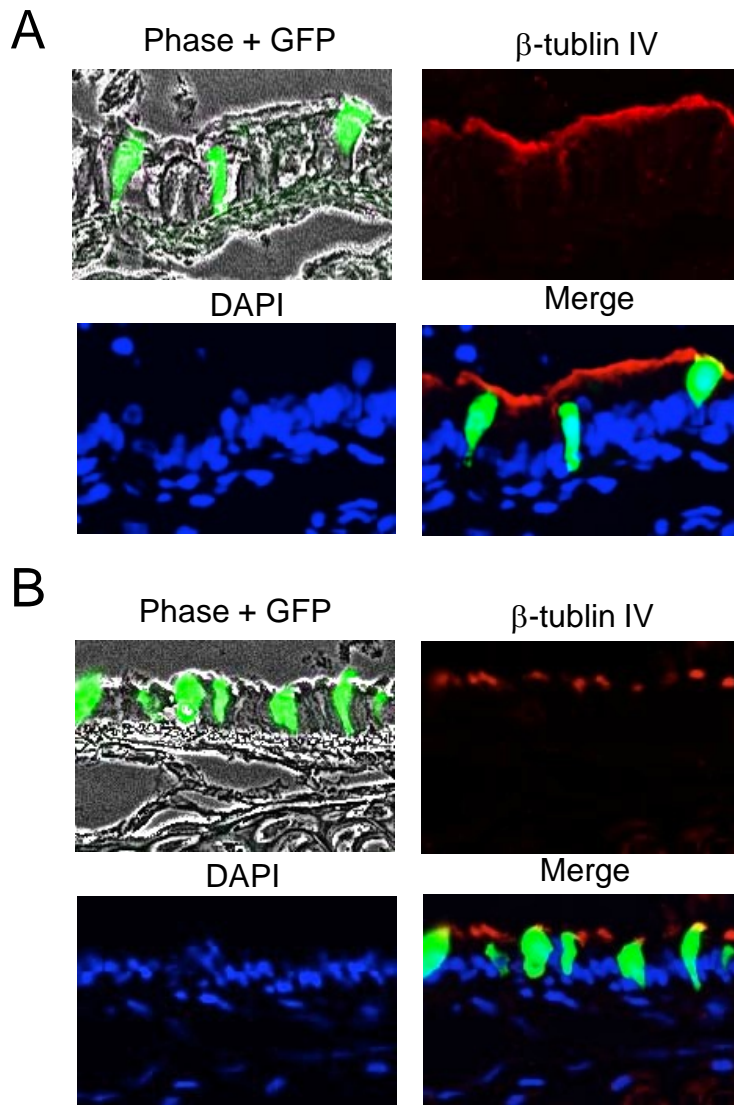


FIG.6

